Nonhelical Inverse Transfer of a Decaying Turbulent Magnetic Field

Axel Brandenburg,[1,2,*] Tina Kahniashvili,[3,4,5,†] and Alexander G. Tevzadze[6,‡]

[1]Nordita, KTH Royal Institute of Technology and Stockholm University, Roslagstullsbacken 23, 10691 Stockholm, Sweden
[2]Department of Astronomy, AlbaNova University Center, Stockholm University, 10691 Stockholm, Sweden
[3]The McWilliams Center for Cosmology and the Department of Physics, Carnegie Mellon University, 5000 Forbes Avenue, Pittsburgh, Pennsylvania 15213, USA
[4]Department of Physics, Laurentian University, Ramsey Lake Road, Sudbury, Ontario P3E 2C, Canada
[5]Abastumani Astrophysical Observatory, Ilia State University, 3-5 Cholokashvili Avenue, Tbilisi GE-0194, Georgia
[6]Faculty of Exact and Natural Sciences, Tbilisi State University, 1 Chavchavadze Avenue, Tbilisi 0128, Georgia

(Received 8 April 2014; published 19 February 2015)

In the presence of magnetic helicity, inverse transfer from small to large scales is well known in magnetohydrodynamic (MHD) turbulence and has applications in astrophysics, cosmology, and fusion plasmas. Using high resolution direct numerical simulations of magnetically dominated self-similarly decaying MHD turbulence, we report a similar inverse transfer even in the absence of magnetic helicity. We compute for the first time spectral energy transfer rates to show that this inverse transfer is about half as strong as with helicity, but in both cases the magnetic gain at large scales results from velocity at similar scales interacting with smaller-scale magnetic fields. This suggests that both inverse transfers are a consequence of universal mechanisms for magnetically dominated turbulence. Possible explanations include inverse cascading of the mean squared vector potential associated with local near two dimensionality and the shallower k^2 subinertial range spectrum of kinetic energy forcing the magnetic field with a k^4 subinertial range to attain larger-scale coherence. The inertial range shows a clear k^{-2} spectrum and is the first example of fully isotropic magnetically dominated MHD turbulence exhibiting weak turbulence scaling.

DOI: 10.1103/PhysRevLett.114.075001 PACS numbers: 94.05.Lk, 96.50.Tf

The nature of magnetohydrodynamic (MHD) turbulence has received significant attention in recent years [1]. Whenever plasma is ionized, it is electrically conducting and Kolmogorov's turbulence theory [2] has to be replaced by an appropriate theory for MHD turbulence [3]. This becomes relevant under virtually all astrophysical circumstances. However, the universal character of MHD turbulence is debated and several fundamental questions remain unanswered: what do kinetic and magnetic energy spectra look like and are they similar? How does this depend on the magnetic Prandtl number, $\mathrm{Pr}_M = \nu/\eta$, i.e., the ratio of kinematic viscosity and magnetic diffusivity? What is the role of the Alfvén effect, i.e., how does the presence of a finite Alfvén speed v_A enter the expression for the turbulent energy spectrum?

If the spectral properties of MHD turbulence are governed solely by the rate of energy transfer ϵ, we know from dimensional arguments that the spectrum must scale as $E(k) \sim \epsilon^{2/3} k^{-5/3}$ with wave number k. However, MHD turbulence becomes increasingly anisotropic toward small scales [4], so the spectrum $E(k_\perp, k_\parallel)$ depends on the wave numbers perpendicular and parallel to the magnetic field $\boldsymbol{B}$ and is essentially given by $\epsilon^{2/3} k_\perp^{-5/3}$, so most of the energy cascades perpendicular to $\boldsymbol{B}$.

In the case of forced turbulence, direct numerical simulations (DNS) show similar spectra both with imposed [1] and dynamo-generated [5] fields. However, when $\boldsymbol{B}$ is decaying, the result depends on the value of the initial ratio $v_{\mathrm{A}}/u_{\mathrm{rms}}$ of root-mean-square (rms) Alfvén speed to rms turbulent velocity. Recent DNS [6] found numerical evidence for three different scalings: the Iroshnikov-Kraichnan scaling [7] proportional to $(\epsilon v_A)^{1/2} k^{-3/2}$ for $v_A/u_{\mathrm{rms}} = 0.9$, the Goldreich-Sridhar scaling [4] proportional to $\epsilon^{2/3} k_\perp^{-5/3}$ for $v_A/u_{\mathrm{rms}} = 1.3$, and weak turbulence scaling [8] proportional to $(\epsilon v_A k_\parallel)^{1/2} k_\perp^{-2}$ for $v_A/u_{\mathrm{rms}} = 2.0$; see Ref. [9] for a comparison of these three scalings. However, their physical interpretation is subject to criticism in that the dynamic alignment between $\boldsymbol{u}$ and $\boldsymbol{B}$ can be responsible for the shallower $k^{-3/2}$ scaling [10] and the k^{-2} scaling could also be caused by a dominance of discontinuities [11].

It is usually taken for granted that, for nonhelical turbulence, energy is cascading toward small scales. An inverse cascade has so far only been found for helical turbulence [3,12] and was confirmed in DNS [13–15]. It is evident that this requires significant scale separation, $k_0/k_1 \gg 1$, where k_0 is the wave number of the peak of the spectrum and $k_1 = 2\pi/L$ is the minimal wave number of the domain of size L. Since an inverse transfer was not expected to occur in the absence of helicity, most previous work did not allow for $k_0/k_1 \gg 1$. However, when k_0/k_1 is moderate, some inverse cascading was found [14]. The present Letter shows that this behavior is genuine and more pronounced at higher resolution, larger Reynolds numbers, and larger k_0/k_1.

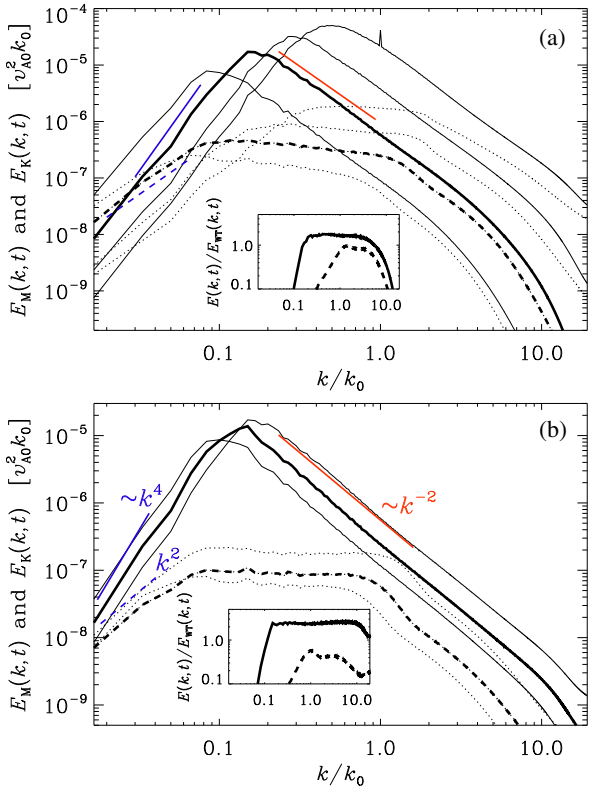

FIG. 1 (color online). (a) Magnetic (solid lines) and kinetic (dashed lines) energy spectra for Run A at times $t/\tau_A = 18$, 130, 450, and 1800; the time $t/\tau_A = 450$ is shown as bold lines. The straight lines indicate the slopes k^4 (solid blue line), k^2 (dashed blue line), and k^{-2} (solid red line). (b) The same for Run B, at $t/\tau_A = 540$, 1300, and 1800, with $t/\tau_A = 1300$ shown as bold lines. The insets show E_M and E_K compensated by $E_{\rm WT}$.

We solve the compressible MHD equations for $\boldsymbol{u}$, the gas density ρ at constant sound speed c_s, and the magnetic vector potential $\boldsymbol{A}$, so $\boldsymbol{B} = \nabla \times \boldsymbol{A}$. Following our earlier work [16–18], we initialize our decaying DNS by restarting them from a snapshot of a driven DNS, where a random forcing was applied in the evolution equation for $\boldsymbol{A}$ rather than $\boldsymbol{u}$ [19]. To allow for sufficient scale separation, we take $k_0/k_1 = 60$. We use the PENCIL CODE [29] at a resolution of 2304^3 mesh points on 9216 processors. The code uses sixth order finite differences and a third order accurate time stepping scheme.

Our magnetic and kinetic energy spectra are normalized such that $\int E_M(k,t)dk = \mathcal{E}_M(t) = v_A^2/2$ and $\int E_K(k,t)dk = \mathcal{E}_K(t) = u_{\rm rms}^2/2$ are magnetic and kinetic energies per unit mass. The magnetic integral scale is defined as $\xi_M = k_M^{-1}(t) = \int k^{-1} E_M(k,t)dk/\mathcal{E}_M(t)$. Time is given in initial Alfvén times $\tau_A = (v_{A0}k_0)^{-1}$, where $v_{A0} = v_A(0)$. In Fig. 1 we show $E_M(k,t)$ and $E_K(k,t)$ for Runs A and B (restarted from A at $t/\tau_A = 450$) with $\mathrm{Pr}_M = 1$ and 10, respectively, and in Fig. 2 slices $B_z(x,y)$ and $u_z(x,y)$ at $z = 0$ at the last time Run A. We find an inertial range with weak turbulence scaling,

$$E_{\rm WT}(k,t) = C_{\rm WT}(\epsilon v_A k_M)^{1/2} k^{-2}, \quad (1)$$

where $k_M^{-1}(t) = \int k^{-1} E_M(k,t)dk/\mathcal{E}_M(t)$ is the integral scale and k_M has been used in place of $k_\parallel$. The prefactor is $C_{\rm WT} \approx 1.9$ for $\mathrm{Pr}_M = 1$ and ≈ 2.4 for $\mathrm{Pr}_M = 10$; see the insets. In agreement with earlier work [3,17], $\mathcal{E}_M$ decays like t^{-1}.

At small wave numbers the k^4 and k^2 subinertial ranges, respectively, for $E_M(k,t)$ and $E_K(k,t)$ are carried over from the initial conditions. The k^4 Batchelor spectrum is in agreement with the causality requirement [30,31] for the divergence-free vector field $\boldsymbol{B}$. The velocity is driven entirely by the magnetic field (no kinetic forcing) and follows a white noise spectrum, $E_K(k) \propto k^2$ [31]. The resulting difference in the scaling implies that, although magnetic energy dominates over kinetic, the two spectra must cross at sufficiently small wave numbers. This idea may also apply to incompressible [32] and relativistic [33]

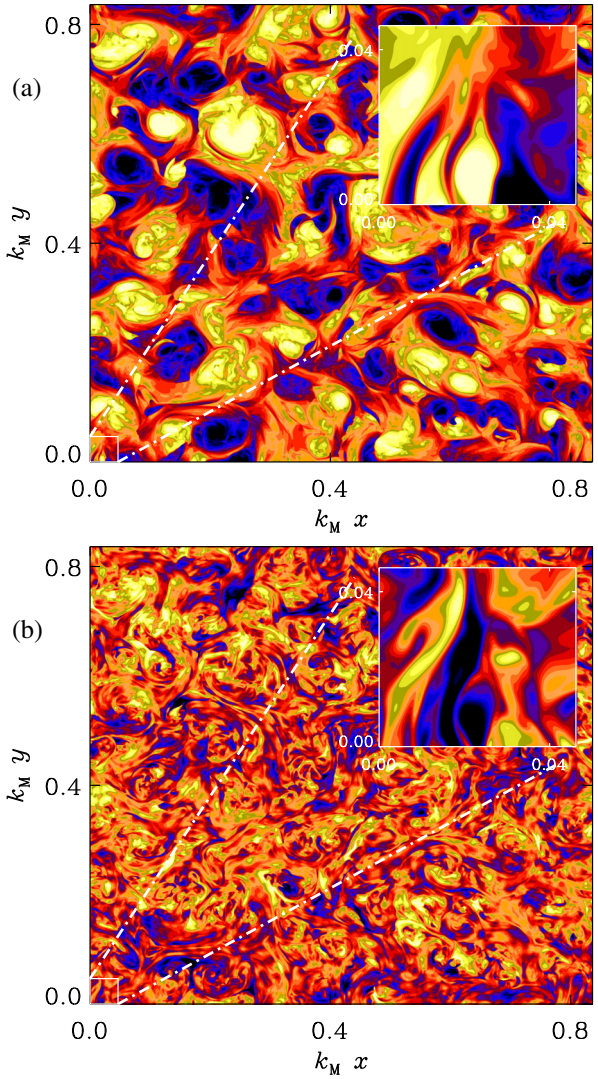

FIG. 2 (color online). Contours of (a) $B_z(x,y)$ and (b) $u_z(x,y)$ for Run A. The insets show a zoom into the small square in the lower left corner.

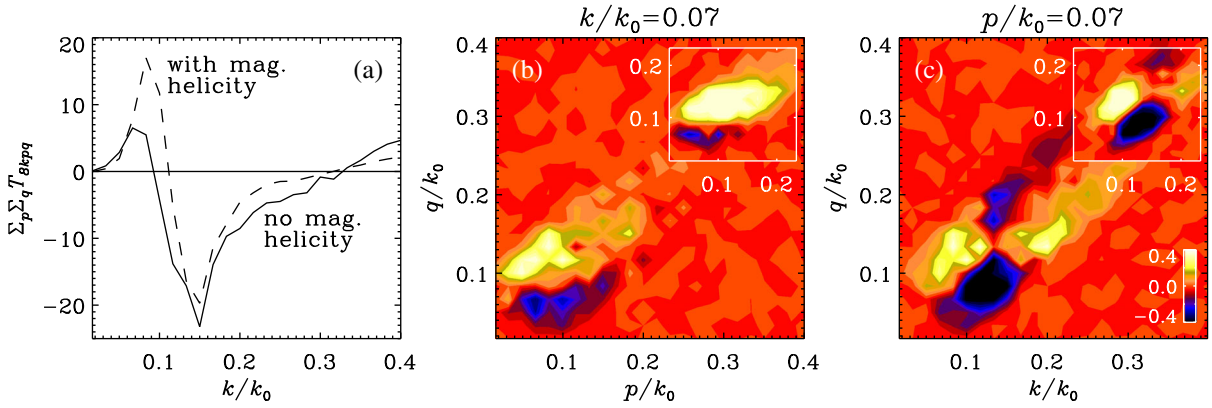

FIG. 3 (color online). Spectral transfer function T_{kpq}, (a) as a function of k and summed over all p and q, (b) as a function of p and q for $k/k_1 = 4$, and (c) as a function of k and q for $p/k_1 = 4$. The dashed line in (a) and the insets in (b) and (c) show the corresponding case for a DNS with helicity, both for Pr_M.

simulations, where inverse nonhelical transfer has recently been confirmed.

To quantify the nature of inverse transfer we show in Fig. 3 representations of the spectral transfer function $T_{kpq} = \langle \boldsymbol{J}^k \cdot (\boldsymbol{u}^p \times \boldsymbol{B}^q) \rangle$ and compare it with the corresponding helical case of Ref. [18], but with 1024^3 mesh points and at a comparable time. Here, the superscripts indicate the radius of a shell in wave number space of Fourier filtered vector fields; see Ref. [15] for such an analysis in driven helical turbulence. The transfer function T_{kpq} quantifies the gain of magnetic energy at wave number k from interactions of velocities at wave number p and magnetic fields at wave number q. Figure 3(a) shows a gain for $k/k_0 < 0.1$, which is about half of that for the helical case. The corresponding losses for $k/k_0 > 0.1$ are about equal in the two cases. In both cases, the magnetic gain at $k/k_0 = 0.07 = 4/60$ results from $\boldsymbol{u}^p$ with $0 < p/k_0 < 0.2$ interacting with $\boldsymbol{B}^q$ at $q/k_0 > 0.1$; see the light yellow shades in Fig. 3(b). Note that work done by the Lorentz force is $\langle \boldsymbol{u}^p \cdot (\boldsymbol{J}^k \times \boldsymbol{B}^q) \rangle = -T_{kpq}$. Thus, negative values of T_{kpq} quantify the gain of *kinetic* energy at wave number p from interactions of magnetic fields at wave numbers k and q. The blue dark shades in Fig. 3(c) indicate, therefore, that the gain of kinetic energy at $p/k_0 = 0.07$ results from magnetic interactions at wave numbers k and q of around $0.1k_0$. These results support the interpretation that the increase of spectral power at large scales is similar to the inverse transfer in the helical case; see Ref. [19] for information concerning the *total* energy transfer.

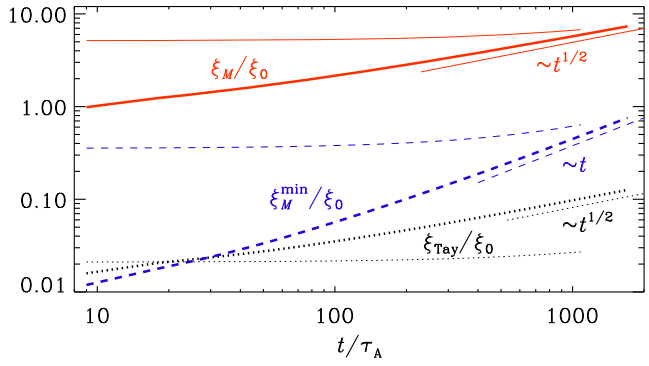

FIG. 4 (color online). Time evolution of $\xi_M = k_M^{-1}$ and $\xi_M^{\rm min}$, as well as the Taylor microscale $\xi_{\rm Tay}$. Fat (thin) lines are for Run A (B).

To exclude the possibility that the inverse energy transfer is a consequence of the invariance of magnetic helicity, $\mathcal{H}_M(t) = \langle \boldsymbol{A} \cdot \boldsymbol{B} \rangle$, we compare ξ_M with its lower bound $\xi_M^{\rm min} = |\mathcal{H}_M|/2\mathcal{E}_M$ [17]; see Fig. 4. In nonhelical MHD turbulence, ξ_M is known to grow like $t^{1/2}$ [3,17]. Even though the initial condition was produced with nonhelical plane wave forcing, we find $\mathcal{H}_M \neq 0$ due to fluctuations. Since $\mathcal{H}_M$ is conserved and $\mathcal{E}_M$ decays like t^{-1} [3,17], $\xi_M^{\rm min}$ grows linearly and faster than $\xi_M \sim t^{1/2}$, so they will meet at $t/\tau_A = 10^5$ and then continue to grow as $t^{-2/3}$ [3,17], but at $t/\tau_A = 10^3$ this cannot explain the inverse transfer. By contrast, we cannot exclude the possibility of the quasi-two-dimensional mean squared vector potential, $\langle A_{\rm 2D}^2 \rangle$, being approximately conserved [19]. This could explain the $\xi_M \sim t^{1/2}$ scaling and the inverse transfer if the flow was locally two dimensional [34].

Since $u_{\rm rms}$, v_A, and k_M are all proportional to $t^{-1/2}$, the decay is self-similar in such a way that the Reynolds and Lundquist numbers, $\mathrm{Re} = u_{\rm rms}/\nu k_M$ and $\mathrm{Lu} = v_A/\eta k_M$, remain constant. Since $\mathcal{E}_K \ll \mathcal{E}_M$, the dissipated energy comes predominantly from $-d\mathcal{E}_M/dt$, and yet a substantial

TABLE I. Comparison of relative dissipation rates, energies, and other parameters for the two simulations discussed.

Run	P_M	v_{A0}/c_s	$u_{\rm rms}/v_A$	Lu	Re	ϵ_K/ϵ_M	ϵ_M/ϵ	ϵ_K/ϵ
A	1	0.15	0.36	700	230	0.52	0.66	0.34
B	10	0.03	0.21	6300	130	0.93	0.52	0.48

fraction of it is used to drive kinetic energy by performing work on the Lorentz force. Nevertheless, the viscous to magnetic dissipation ratio ϵ_K/ϵ_M increases only by a factor of 1.8 as Pr_M increases from 1 to 10; see Table I. This is less than for kinetically driven MHD turbulence, where $\epsilon_K/\epsilon_M \propto \mathrm{Pr}_M^n$ with $n = 0.3$–0.7 [35]. Therefore, ϵ_M is here larger than in driven MHD turbulence, where large Lu can still be tolerated. This suggests that Run B may be under-resolved, which might also explain why it did not reach asymptotic scaling in Fig. 4.

In summary, we have shown that inverse transfer is a ubiquitous phenomenon of both helical and nonhelical MHD. For helical MHD, this has been well known for nearly four decades [12], but for nonhelical MHD there have only been some low resolution DNS [14,18]. Our DNS confirm an early finding by Olesen [36] that this inverse transfer occurs for all initial spectra that are sufficiently steep. His argument applies to hydrodynamic and MHD turbulence if the two spectra are parallel to each other. In our case, however, owing to the shallower k^2 spectrum of kinetic energy, kinetic energy always dominates over magnetic at large enough length scales. Either this or the near conservation of $\langle \boldsymbol{A}_{\mathrm{2D}}^2 \rangle$ could be responsible for inverse transfer in magnetically dominated turbulence. This process is significant for cosmology and astrophysics [33], with applications not only to primordial magnetic fields, but also to ejecta from young stars, supernovae, and active galactic nuclei [37].

Our results support the idea of the weak turbulence k^{-2} scaling for a strong magnetic field that is here, for the first time, globally isotropic and not an imposed one [38]. At small scales, however, approximate equipartition is still possible. The decay is slower than for the usual MHD turbulence, which is arguably governed by the Loitsyansky invariant [39]. Future investigations of the differences between these types of turbulence are warranted [19]. Interestingly, the extended plateau in the velocity spectrum around the position of the magnetic peak may be important for producing observationally detectable broad gravitational wave spectra [40].

We appreciate the useful discussions with A. Neronov. Computing resources have been provided by the Swedish National Allocations Committee at the Center for Parallel Computers at the Royal Institute of Technology and by the Carnegie Mellon University Supercomputer Center. We acknowledge support from Swedish Research Council Grants No. 621-2011-5076 and No. 2012-5797, European Research Council AstroDyn Project No. 227952, Research Council of Norway FRINATEK Grant No. 231444, Swiss NSF Grant No. SCOPES IZ7370-152581, NSF Grant No. AST-1109180, and NASA Astrophysics Theory Program Grant No. NNXlOAC85G. A. B. and A. T. acknowledge the hospitality of the McWilliams Center for Cosmology.

*brandenb@nordita.org
†tinatin@phys.ksu.edu
‡aleko@tevza.org

[1] W. H. Matthaeus, S. Ghosh, S. Oughton, and D. A. Roberts, J. Geophys. Res. **101**, 7619 (1996); J. Cho and E. T. Vishniac, Astrophys. J. **538**, 217 (2000); J. Maron and P. Goldreich, Astrophys. J. **554**, 1175 (2001).
[2] A. Kolmogorov, Dokl. Akad. Nauk SSSR **30**, 301 (1941).
[3] D. Biskamp and W.-C. Müller, Phys. Rev. Lett. **83**, 2195 (1999).
[4] P. Goldreich and S. Sridhar, Astrophys. J. **438**, 763 (1995).
[5] N. E. L. Haugen, A. Brandenburg, and W. Dobler, Phys. Rev. E **70**, 016308 (2004).
[6] E. Lee, M. E. Brachet, A. Pouquet, P. D. Mininni, and D. Rosenberg, Phys. Rev. E **81**, 016318 (2010).
[7] R. S. Iroshnikov, Sov. Astron. **7**, 566 (1964); R. H. Kraichnan, Phys. Fluids **8**, 1385 (1965).
[8] S. Galtier, S. V. Nazarenko, A. C. Newell, and A. Pouquet, J. Plasma Phys. **63**, 447 (2000).
[9] A. Brandenburg and Å. Nordlund, Rep. Prog. Phys. **74**, 046901 (2011); W. H. Matthaeus, D. C. Montgomery, M. Wan, and S. Servidio, J. Turbul. **13**, N37 (2012).
[10] J. Mason, F. Cattaneo, and S. Boldyrev, Phys. Rev. Lett. **97**, 255002 (2006).
[11] V. Dallas and A. Alexakis, Astrophys. J. **788**, L36 (2014).
[12] A. Pouquet, U. Frisch, and J. Léorat, J. Fluid Mech. **77**, 321 (1976).
[13] D. Balsara and A. Pouquet, Phys. Plasmas **6**, 89 (1999).
[14] M. Christensson, M. Hindmarsh, and A. Brandenburg, Phys. Rev. E **64**, 056405 (2001).
[15] A. Brandenburg, Astrophys. J. **550**, 824 (2001).
[16] T. Kahniashvili, A. Brandenburg, A. G. Tevzadze, and B. Ratra, Phys. Rev. D **81**, 123002 (2010).
[17] A. G. Tevzadze, L. Kisslinger, A. Brandenburg, and T. Kahniashvili, Astrophys. J. **759**, 54 (2012).
[18] T. Kahniashvili, A. G. Tevzadze, A. Brandenburg, and A. Neronov, Phys. Rev. D **87**, 083007 (2013); note that in their Eq. (14), $\boldsymbol{v}/\boldsymbol{\eta}$ should read $\partial \boldsymbol{v}/\partial \boldsymbol{\eta}$.
[19] See Supplemental Material at http://link.aps.org/supplemental/10.1103/PhysRevLett.114.075001 for details regarding the initial conditions, the near conservation of $\langle \boldsymbol{A}_{\mathrm{2D}}^2 \rangle$, the spectral energy transfer function, and other properties of decaying turbulence, which includes Refs. [20–28].
[20] L. Campanelli, Eur. Phys. J. C **74**, 2690 (2014).
[21] C. Kalelkar and R. Pandit, Phys. Rev. E **69**, 046304 (2004).
[22] M. Christensson, M. Hindmarsh, and A. Brandenburg, Phys. Rev. E **64**, 056405 (2001).
[23] J. Baerenzung, H. Politano, Y. Ponty, and A. Pouquet, Phys. Rev. E **77**, 046303 (2008).
[24] A. Sen, P. D. Mininni, D. Rosenberg, and A. Pouquet, Phys. Rev. E **86**, 036319 (2012).
[25] A. Brandenburg, Å. Nordlund, R. F. Stein, and I. Torkelsson, Astrophys. J. **446**, 741 (1995).
[26] A. Brandenburg, Chaos Solitons Fractals **5**, 2023 (1995).
[27] A. Brandenburg, R. L. Jennings, Å. Nordlund, M. Rieutord, R. F. Stein, and I. Tuominen, J. Fluid Mech. **306**, 325 (1996).
[28] S. Sur, L. Pan, and E. Scannapieco, Astrophys. J. **790**, L9 (2014).
[29] See http://pencil-code.googlecode.com/.

[30] R. Durrer and C. Caprini, J. Cosmol. Astropart. Phys. 11 (2003) 010.
[31] P. A. Davidson, *Turbulence* (Oxford University Press, New York, 2004).
[32] A. Berera and M. Linkmann, Phys. Rev. E **90**, 041003(R) (2014).
[33] J. Zrake, Astrophys. J. **794**, L26 (2014).
[34] A. Pouquet, J. Fluid Mech. **88**, 1 (1978).
[35] A. Brandenburg, Astrophys. J. **791**, 12 (2014).
[36] P. Olesen, Phys. Lett. B **398**, 321 (1997).
[37] A. M. Beck, K. Dolag, H. Lesch, and P. P. Kronberg, Mon. Not. R. Astron. Soc. **435**, 3575 (2013).
[38] J. C. Perez and S. Boldyrev, Astrophys. J. Lett. **672**, L61 (2008).
[39] P. A. Davidson, J. Turbul. **1**, N6 (2000).
[40] T. Kahniashvili, L. Campanelli, G. Gogoberidze, Y. Maravin, and B. Ratra, Phys. Rev. D **78**, 123006 (2008).